

THE  
UNIVERSITY  
OF RHODE ISLAND

University of Rhode Island  
DigitalCommons@URI

---

Chemistry Faculty Publications

Chemistry

---

2004

# On the Encapsulation of Nickel Clusters by Molecular Nitrogen

Pablo Nigra  
*University of Rhode Island*

David L. Freeman  
*University of Rhode Island, [dfreeman@uri.edu](mailto:dfreeman@uri.edu)*

*See next page for additional authors*

Follow this and additional works at: [https://digitalcommons.uri.edu/chm\\_facpubs](https://digitalcommons.uri.edu/chm_facpubs)

Terms of Use  
All rights reserved under copyright.

---

## Citation/Publisher Attribution

Nigra, P., Freeman, D. L., Sabo, D. & Doll, J. D. (2004). On the Encapsulation of Nickel Clusters by Molecular Nitrogen. *Journal of Chemical Physics*, 121(1), 475-482. doi: 10.1063/1.1757435  
Available at: <http://dx.doi.org/10.1063/1.1757435>

This Article is brought to you for free and open access by the Chemistry at DigitalCommons@URI. It has been accepted for inclusion in Chemistry Faculty Publications by an authorized administrator of DigitalCommons@URI. For more information, please contact [digitalcommons@etal.uri.edu](mailto:digitalcommons@etal.uri.edu).

---

**Authors**

Pablo Nigra, David L. Freeman, Dubravko Sabo, and J. D. Doll

# On the encapsulation of nickel clusters by molecular nitrogen

Pablo Nigra<sup>a)</sup> and David L. Freeman<sup>b)</sup>

*Department of Chemistry, University of Rhode Island, Kingston, Rhode Island 02881*

Dubravko Sabo and J. D. Doll

*Department of Chemistry, Brown University, Providence, Rhode Island 02912*

(Received 18 February 2004; accepted 9 April 2004)

The structures and energetic effects of molecular nitrogen adsorbates on nickel clusters are investigated using an extended Hückel model coupled with two models of the adsorbate–nickel interaction. The potential parameters for the adsorbates are chosen to mimic experimental information about the binding strength of nitrogen on both cluster and bulk surface phases of nickel. The first model potential is a simple Lennard-Jones interaction that leads to binding sites in holes defined by sets of near-neighbor nickel atoms. The second model potential has a simple three-body form that forces the model nitrogen adsorbates to bind directly to single nickel atoms. Significant rearrangement of the core nickel structures are found in both models. A disconnectivity graph analysis of the potential energy surfaces implies that the rearrangements arise from low transition state barriers and the small differences between available isomers in the nickel core. © 2004 American Institute of Physics. [DOI: 10.1063/1.1757435]

## I. INTRODUCTION

In recent publications Sabo *et al.*<sup>1,2</sup> have examined the effect of encapsulation on the structures of Lennard-Jones clusters. That work has demonstrated that as a function of the binding strength and size between unlike atoms, encapsulation can generate new structures and reorder the energies of core structures. The current publication is an extension of that work to study the effect of weakly bound adsorbates on the core structures of nickel clusters.

A motivation for the current work is the experimental studies by Parks *et al.*<sup>3</sup> who have inferred the structures of nickel clusters by the adsorption of molecular nitrogen. In these nitrogen uptake experiments, by monitoring the amount of nitrogen adsorbed, the number of binding sites can be determined. By the examination of reasonable candidate structures, the number of binding sites can help determine the structures of the bare nickel clusters. In separate work Parks *et al.*<sup>4</sup> have found that the binding energy of molecular nitrogen on nickel clusters for most cluster sizes is about 0.75 eV, near the 0.3–0.5 eV adsorption energy experimentally determined for the binding of molecular nitrogen on bulk nickel surfaces.<sup>5</sup> Using an extended Hückel model parameterized to *ab initio* and experimental information, Curotto *et al.*<sup>6</sup> have examined the isomer distributions of bare nickel clusters and have found that the differences between adjacent isomers are as small as 0.05 eV. The origin of the small energy differences appears to be Jahn–Teller distortions, and the high density of low energy minima may be correct even though the details of the potential model itself is not quantitatively accurate. Because the differences in energy between adjacent isomers may be small compared to the

binding energy of nitrogen molecules on nickel clusters, it is natural to ask to what extent the adsorption of the molecular nitrogen might perturb the structures of the nickel core. In the current work, we address the extent of perturbation of the core nickel structures using two potential models. For both models, the interaction potential between the nickel atoms is taken to be the same extended Hückel model used previously.<sup>6</sup> For the interaction between the nitrogen molecules and the nickel atoms in the cluster, we seek the simplest possible potentials that can be expected to provide some physical insight. The interaction potential between the nitrogen adsorbates and the nickel atoms is taken to be first a Lennard-Jones potential with a binding strength of about 0.5 eV. Because the nitrogen molecules in the spherical Lennard-Jones model tend to bind to hole binding sites in contrast to the expected behavior for molecular nitrogen,<sup>4</sup> as a second model we use a nitrogen–nickel interaction with a modified three-body type Lennard-Jones interaction that is sufficiently directional that the nitrogen molecules bind directly on the nickel atoms. While it would be presumptuous to claim that our results are quantitative, we can at least address the kinds of effects to be expected in the nitrogen uptake experiments.

The contents of the remainder of this paper are as follows. In Sec. II, we review the potential models used and discuss the methods employed to find the global minima and isomer distributions for each cluster size. We also discuss the methods used to locate transition state structures that help in the analysis of the results. In Sec. III, we present our results for Ni<sub>7</sub> with up to seven adsorbates in the two potential models used, and in Sec. IV we discuss the implications of our studies.

## II. METHOD

The interaction between the nickel atoms is taken from the extended Hückel model with the same parameters developed by Curotto *et al.*<sup>6</sup> We make no effort to review the

<sup>a)</sup>Present address: Department of Chemistry, Oregon State University, Corvallis, OR 97331.

<sup>b)</sup>Author to whom correspondence should be addressed. Electronic mail: freeman@chm.uri.edu

TABLE I. The Lennard-Jones parameters used in model 1.

Species	$\epsilon$ (K)	$\sigma$ (Å)
N <sub>2</sub> -N <sub>2</sub>	91.5	3.681
N <sub>2</sub> -Ni	1448.2	3.709

details of the implementation of the extended Hückel method here. For the interactions between the nitrogen molecules, we use the standard Lennard-Jones potential. We have chosen two models for the interaction between the nitrogen molecules and the nickel atoms. In the first of these models (hereafter referred to as “model 1”), we again use the standard Lennard-Jones model

$$v_{\text{LJ}}(r) = 4\epsilon \left[ \left( \frac{\sigma}{r} \right)^{12} - \left( \frac{\sigma}{r} \right)^6 \right], \quad (1)$$

where  $\sigma$  and  $\epsilon$  are, respectively, the usual length and energy parameters and  $r$  is the distance between a nitrogen molecule (assumed spherical) and a nickel atom. The specific Lennard-Jones parameters for this first model along with the parameters for the nitrogen–nitrogen interactions are given in Table I. The interaction parameters between the nitrogen and nickel atoms are taken so that the binding energy of a single adsorbate on Ni<sub>7</sub> in the lowest energy point on the potential surface is about 0.5 eV. The Ni–N<sub>2</sub> length parameter is the arithmetic mean of the N<sub>2</sub>–N<sub>2</sub>  $\sigma$  parameter and the equivalent  $\sigma$  parameter taken from the bond length of Ni<sub>2</sub> as predicted by the extended Hückel model.

Using model 1, we can observe the effect of spherical encapsulating adsorbates on the underlying structures of the nickel core. As discussed below, this spherical Lennard-Jones model results in multiple nickel atom adsorption sites. From studies of the adsorption of molecular nitrogen on nickel surfaces,<sup>7</sup> it is believed that nitrogen adsorbs directly on the nickel atoms owing to interactions between nickel and the lone pairs on N<sub>2</sub>. Perhaps the simplest directional function that we can choose contains an angular dependence of the form  $\cos^n \theta$ , where  $n$  is some even power. This angular function becomes more sharply directional as  $n$  is increased. To retain this simplicity of form, we introduce a second model (hereafter referred to as “model 2”) that binds the adsorbates directly on the nickel atoms using a three-body potential of the form

$$v_{3b}(\mathbf{r}_1, \mathbf{r}_2, \mathbf{r}_3) = 4\epsilon_{3b} \left[ \left( \frac{\sigma}{r} \right)^{12} - \left( \frac{\sigma}{r} \right)^6 \cos^4 \theta \right], \quad (2)$$

where  $\mathbf{r}_1$  and  $\mathbf{r}_2$  are the coordinates of any two pairs of nickel atoms,  $\mathbf{r}_3$  is the coordinate of the model nitrogen molecule (again assumed to be spherical),  $r$  is the distance between the midpoint of the line connecting the two nickel atoms with the coordinate of the nitrogen molecule, and  $\theta$  is the angle between the line connecting the two nickel atoms and the line between the midpoint of the line connecting the two nickel atoms with the coordinate of the nitrogen molecule (see Fig. 1). As is made clear by the data to be presented shortly, this three-body potential with suitable parameters binds the nitrogen molecules directly to the nickel atoms. The length parameters chosen in this work are iden-

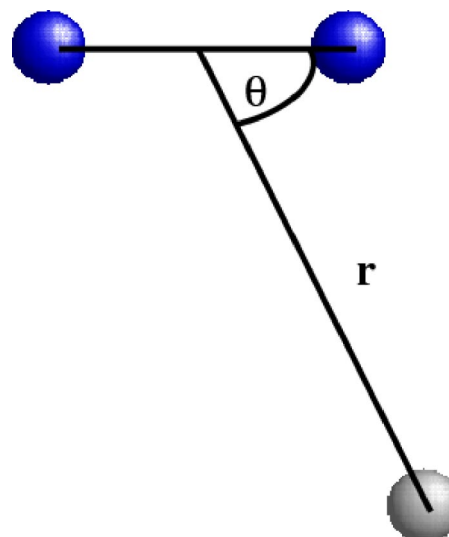


FIG. 1. The dark spheres represent nickel atoms and the light sphere represents a nitrogen molecule. This same shading scheme is used in all subsequent figures. The coordinates  $r$  and  $\theta$  are those used in Eq. (2).

tical to the Lennard-Jones length parameters given in Table I. The nitrogen–nitrogen interactions are assumed to be the identical spherical Lennard-Jones model used in the first case. The only new parameter is  $\epsilon_{3b}$  in Eq. (2) which is chosen to be 2619.6 K, a value that binds N<sub>2</sub> to Ni<sub>7</sub> with an energy of about 0.6 eV.

Using both models 1 and 2, we then explore the potential energy surface for a core of seven nickel atoms and from one to seven nitrogen molecules. In the case of model 2, the seven adsorbates take the system to saturation. Our goals in exploring the potential energy surfaces using each model include determining if there are reorderings of the core structures for bare Ni<sub>7</sub> by the adsorbates as well as seeking the existence of new core structures. We also attempt to infer information about the isomerization dynamics of the system. In that regard, we seek both the low-lying potential energy minima as well as some of the important transition states.

To find the low lying minima, we use several methods both to generate and verify the minima. Our principal method is the basin hopping approach.<sup>8</sup> In basin hopping, the actual potential energy surface of a system is replaced by a surface defined so that every configuration within the basin of a potential minimum has the same energy as the minimum configuration itself. The basin of a particular potential minimum is defined to be the set of configurations from which the minimum is reached via some quench procedure. Monte Carlo moves in this modified surface easily overcome any barriers that separate the minima, and both the local and global minima of a potential surface are discovered efficiently using such a Monte Carlo walk. As originally applied<sup>8</sup> to potential functions constructed from pairwise additive forces, to enhance the efficiency of the basin hopping approach, periodically an atom having a pair energy higher than some fraction of the energy of the atom having the lowest pair energy is rotated randomly about the center of mass of the cluster. Because the model used in the current work contains many-body extended Hückel forces as well as

three-body interactions, an alternative method is required. In this work, when attempting a rotation, we temporarily represent the interactions between all particles with Lennard-Jones pairwise forces, and with that configuration, use the same pair energy criterion to choose which atom to rotate. The energy of the rotated configuration is then computed with the correct potential. The quenches to the nearest local minimum in the basin hopping approach are executed using the Fletcher-Reeves-Polak-Ribiere version of the conjugate gradient method using the algorithm given in *Numerical Recipes*.<sup>9</sup> To verify each structure is a true local (or global) minimum, we further quench the structures using molecular dynamics on the potential surface with an added dissipative frictional force. In all cases, we are able to quench the energy of the structures to at least five significant figures. We initiate each basin hopping search from a random configuration, and repeat the procedure with new random starting points using from 200 to 1000 trajectories.

With the located potential minima, we then seek the transition state barriers connecting the various minima using the variant of the eigenvector following method discussed by Tsai and Jordan.<sup>10</sup> Although we apply the eigenvector following method roughly as in the original publication, we modify the overall procedure slightly so that we can verify the transition states located as well as discover a few additional potential minima not found in the original basin hopping search. To apply the eigenvector following method, we begin the search at any one of the potential surface minima discovered using basin hopping. We then construct the Hessian matrix using analytic first derivatives with numerical second derivatives. For the nickel-nickel potential, the method to obtain the analytic first derivatives is discussed in Ref. 5. We then follow the paths generated by the eigenvectors of the Hessian in the usual fashion until we either locate a transition state or execute so many iterations in the procedure that we are convinced that for that eigenvector, the procedure is not convergent. We verify that we have located a transition state by diagonalization of the Hessian and confirmation that there is exactly one negative eigenvalue. Because of the weak binding in the systems under study, it is necessary to discriminate between small negative eigenvalues associated with rotational modes and those associated with true weak vibrational modes. To distinguish these two possibilities, we form the Hessian using all  $3N$  degrees of freedom ( $N$  is the number of atoms in the cluster) as well as a Hessian with  $3N-6$  degrees of freedom formed by projection of the rotational and center-of-mass translational degrees of freedom as discussed elsewhere.<sup>11,12</sup> We then require that the lowest eigenvalue in magnitude obtained from the projected Hessian agree with one of the eigenvalues of the unprojected Hessian to at least five significant figures. We associate eigenvalues smaller than this lowest projected eigenvalue with the free translations and rotations of the cluster. Of course, we also verify that there are six such near zero eigenvalues. When agreement to five significant figures is not possible, we then quench the structure of the cluster for additional cycles to further refine the structure.

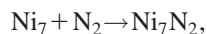
We find the minima connected by a particular transition state by following the eigenvector associated with the nega-

tive eigenvalue in two directions from the transition state for a small step followed by conjugate gradient to the nearest local minimum. In most cases, one of the two minima reached with the conjugate gradient step is the same as the original minimum used to locate the transition state. However, we have found cases where a transition state located from a given potential minimum connects two other minima when conjugate gradient methods are used. To display the resulting potential energy surface information, we construct the associated disconnectivity graphs.<sup>13,14</sup>

### III. RESULTS

We begin the current study by examining again the structures of the bare nickel clusters. In the work of Curotto *et al.*<sup>6</sup> the structures have been determined using a combination of a genetic algorithm<sup>15,16</sup> and Brownian quenches.<sup>17</sup> Using the basin hopping and eigenvector following methods in the current work, we have discovered several structures for bare Ni<sub>7</sub> not found in the original publication. For completeness, we display all discovered bare Ni<sub>7</sub> structures in Fig. 2 and give the respective energies in Table II. The notation to identify each structure used here is the same as that used by Curotto *et al.*;<sup>6</sup> i.e.,  $7.n$  represents the  $n$ th isomer of Ni<sub>7</sub>. The individual isomers are identified only by their energy, and structures having chiral isomers are not displayed or identified separately. Some examples of isomers not found in the previous work are isomer 7.6, which can be viewed as a distortion of structure 7.1, and structures 7.26–7.28 that are similar to isomer 7.24 but with different placements of the atoms in a near planar configuration. Although structures 7.24 and 7.26–7.28 appear planar in the figure, the structures are in fact distorted out of the plane. From Table II we see that, as previously noted, the gaps in energy between adjacent isomers are about 0.05 eV or less.

We next examine the structures obtained using model 1. For the adsorbed structures, we express the energy as the binding energy of the adsorbate to structure 7.1; i.e., the energy change for the zero-temperature process,



so that the zero of energy is represented by structure 7.1 and the nitrogen molecule at infinite separation from each other. In Fig. 3 we show the six structures of a single adsorbate on Ni<sub>7</sub> that have been discovered to be lowest in energy. The binding energy of the single adsorbate is 0.4944 eV, and the energy gaps between the adjacent isomers are on the order of 0.01 eV. These gaps are even smaller than the gaps observed in bare Ni<sub>7</sub>. The lowest energy isomer has a nickel core identical to the lowest energy nickel structure found in the bare system; i.e., structure 7.1. For the higher energy isomers, there is some reordering of structures compared to those observed in Ni<sub>7</sub>. In Fig. 3 the second isomer has a nickel core of structure 7.5 in the bare nickel cluster. The third and fourth isomers do match the third and fourth isomers in bare Ni<sub>7</sub> while the fifth isomer places the adsorbate in a different location relative to the core than the fourth isomer and results in significant distortion of the core. The sixth isomer has a core that matches structure 7.1 but with a

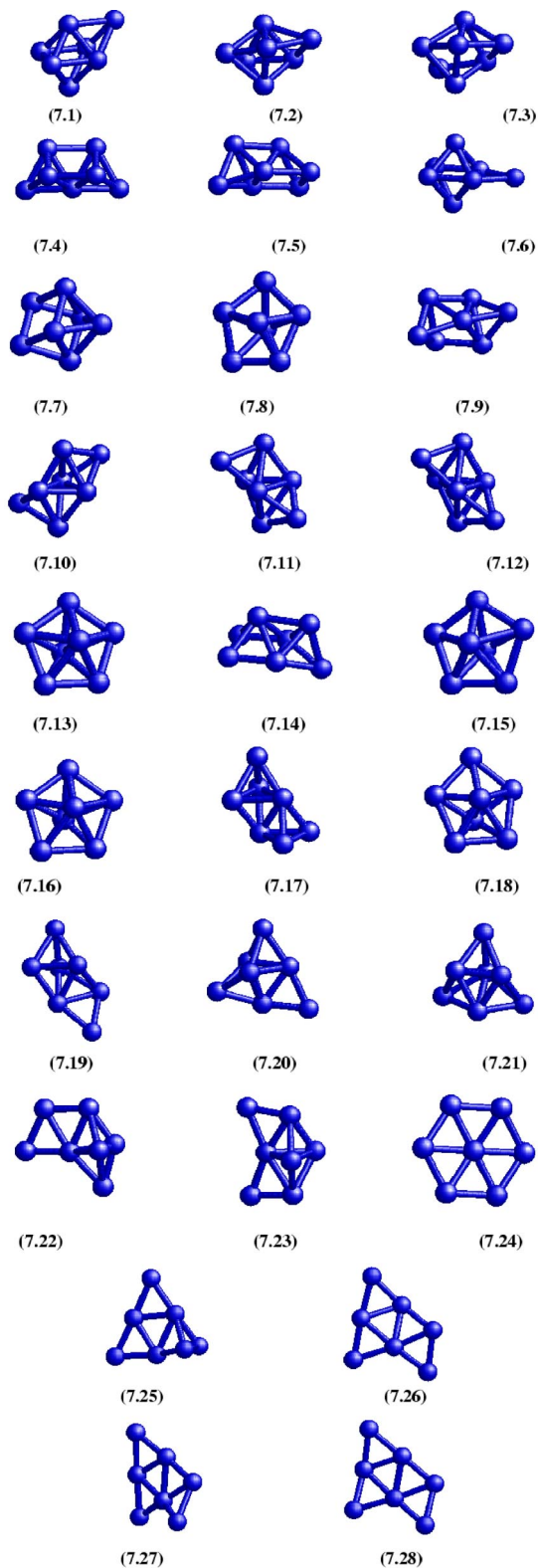


FIG. 2. The structures of bare  $\text{Ni}_7$ . The energies corresponding to each structure are given in Table II. Structures 3, 8, 9, 10, 11, 12, 15, 19, 26, 27, and 28 have chiral isomers that are not displayed.

different placement of the adsorbate relative to the core. In all cases, the adsorbed atom is located in a hole site and not bound directly to any one nickel atom.

In Fig. 4 we show the six lowest energy structures for  $\text{Ni}_7$  with two adsorbates using model 1. In the case of two

TABLE II. The total energies of all discovered isomers for  $\text{Ni}_7$  in the extended Hückel model.

Cluster	Total energy (eV)
7.1	-17.4335
7.2	-17.3851
7.3	-17.3473
7.4	-17.3250
7.5	-17.3064
7.6	-17.3014
7.7	-17.2871
7.8	-17.2837
7.9	-17.2620
7.10	-17.2234
7.11	-17.1914
7.12	-17.1902
7.13	-17.1886
7.14	-17.1851
7.15	-17.1850
7.16	-17.1764
7.17	-17.1544
7.18	-17.1398
7.19	-16.9582
7.20	-16.9434
7.21	-16.9250
7.22	-16.7783
7.23	-16.6258
7.24	-16.4594
7.25	-16.3338
7.26	-15.9435
7.27	-15.9345
7.28	-15.9143

adsorbates, the lowest energy core structure is structure 7.4 in the bare nickel atom system. It is not until the fourth lowest energy isomer depicted in Fig. 4 that structure 7.1 for the bare  $\text{Ni}_7$  cluster appears. As with a single adsorbate, the gaps between adjacent energy isomers are small, and the adsorbed atoms bind to hole sites.

In Fig. 5 we present representations of the lowest energy structures of  $\text{Ni}_7$  with 3–7 adsorbates. In all cases the lowest energy structures for the nickel core do not match structure

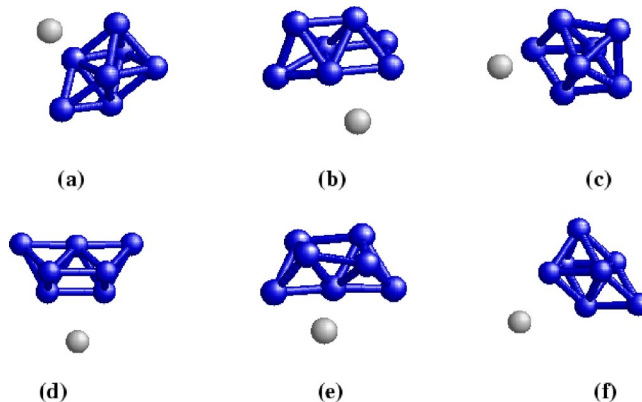


FIG. 3. The structures of  $\text{Ni}_7$  with a single adsorbate using model 1. The structures are given in increasing energy order. The binding energies of the adsorbate for each structure relative to  $\text{Ni}_7$  with the adsorbate at infinite separation are (a) 0.4944 eV, (b) 0.4909 eV, (c) 0.4808 eV, (d) 0.4607 eV, (e) 0.4508 eV, and (f) 0.4338 eV. The small gaps between isomers are on the order of 0.01 eV.

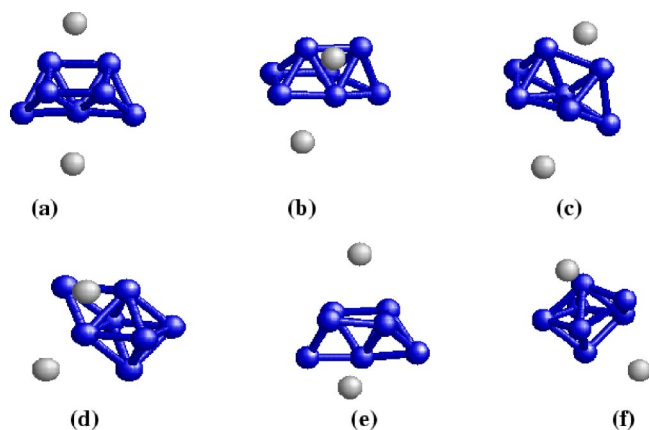


FIG. 4. The structures of  $\text{Ni}_7$  with two adsorbates using model 1. The structures are given in increasing energy order. The binding energies of the two adsorbates for each structure relative to  $\text{Ni}_7$  with both adsorbates at infinite separation are (a) 1.0119 eV, (b) 1.0012 eV, (c) 1.0011 eV, (d) 0.9815 eV, (e) 0.9436 eV, and (f) 0.9370 eV.

7.1 for bare  $\text{Ni}_7$ . As before, each cluster size has many isomers with gaps as small as those found with one or two adsorbates. To preserve space, we do not show the detailed structures for the collection of isomers, but we do give the binding energies of some of the lowest energy isomers in Table III. In Table III, Cluster 10.1 represents the first isomer in energy containing  $\text{Ni}_7$  with three adsorbates (a total of ten atoms), 10.2 represents the second isomer in energy containing  $\text{Ni}_7$  with three adsorbates, and so on.

From the small energy differences between the isomers, it is evident that minor changes in the potential parameters can be expected to lead to differences in the energy orderings of the isomers. However, model 1 may not be physically reasonable for nitrogen adsorption. It is believed that molecular nitrogen binds to bulk nickel surfaces perpendicular to the plane of the surface atop the nickel atoms.<sup>7</sup> To test the sensitivity of the results just presented to the geometric constraints expected from the binding of molecular nitrogen on nickel, we next present the results obtained using model 2.

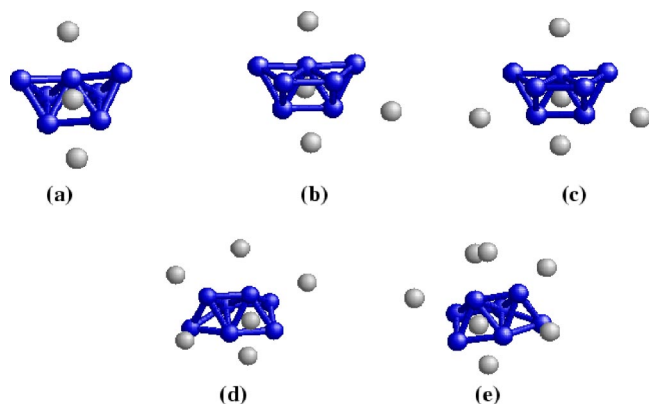


FIG. 5. The lowest energy structures of  $\text{Ni}_7$  with, respectively, 3–7 adsorbate atoms using model 1. None of the core nickel structures match structure 7.1 in bare  $\text{Ni}_7$ . The energies of each cluster relative to bare  $\text{Ni}_7$  and all adsorbates at infinity are (a) 1.5458 eV, (b) 1.9754 eV, (c) 2.4053 eV, (d) 2.8061 eV, and (e) 3.1560 eV.

TABLE III. The binding energies of some of the lowest energy isomers for the larger cluster sizes using model 1.

Cluster	Binding energy (eV)
10.1	1.5458
10.2	1.5026
10.3	1.4396
10.4	1.4314
11.1	1.9754
11.2	1.9358
11.3	1.9337
11.4	1.9112
12.1	2.4053
12.2	2.3706
12.3	2.3693
12.4	2.3419
13.1	2.8061
13.2	2.8057
13.3	2.7723
13.4	2.7383
14.1	3.1560
14.2	3.1551
14.3	3.1478
14.4	3.1399

The structures of  $\text{Ni}_7$  with a single adsorbate in model 2 are represented in Fig. 6. The nickel core for the lowest energy isomer matches structure 7.1 found in bare  $\text{Ni}_7$ . The energy gap between the lowest energy isomer and the isomer next in energy is larger than found in model 1, and the adsorbate binding site is directly on a nickel atom as expected for molecular nitrogen. The first and fourth isomers both have the lowest energy bare  $\text{Ni}_7$  core structure, with the adsorbate binding to atoms in different positions in the two cases. The isomer second lowest in energy [structure (b)] matches structure 7.4 in  $\text{Ni}_7$ .

The structures of  $\text{Ni}_7$  with two adsorbates in model 2 are given in Fig. 7. The nickel core of the second lowest energy isomer [structure (b)] has the configuration of the global minimum for  $\text{Ni}_7$  with structure (a) having a core that matches structure 7.4 for  $\text{Ni}_7$ . The remaining four structures

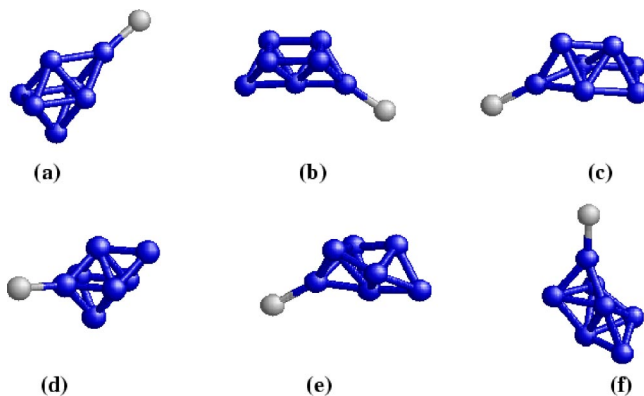


FIG. 6. The structures of  $\text{Ni}_7$  with a single adsorbate using model 2. The structures are given in increasing energy order. The binding energies of the adsorbate for each structure relative to  $\text{Ni}_7$  with the adsorbate at infinite separation are (a) 0.6038 eV, (b) 0.4528 eV, (c) 0.4360 eV, (d) 0.3804 eV, (e) 0.3605 eV, and (f) 0.3576 eV. The energy gap between the lowest energy isomer and the isomer next highest in energy is greater than the gap found in model 1.

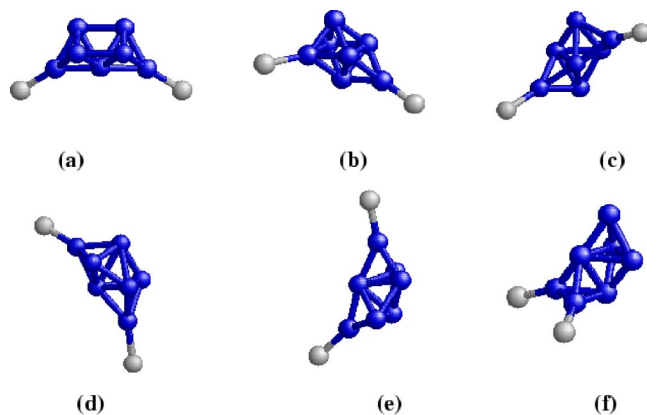


FIG. 7. The structures of  $\text{Ni}_7$  with two adsorbates using model 2. The structures are given in increasing energy order. The binding energies of the adsorbates for each structure relative to  $\text{Ni}_7$  with the adsorbates at infinite separation are (a) 1.0147 eV, (b) 0.9828 eV, (c) 0.9632 eV, (d) 0.9225 eV, (e) 0.9223 eV, and (f) 0.7926 eV.

have the same nickel core but with different placements of the adsorbates. As with a single adsorbate, both adsorbates bind directly to nickel atoms in model 2.

The structures of  $\text{Ni}_7$  with 3–7 adsorbates in model 2 that are lowest in energy are given in Fig. 8. With the exception of structure (e) that contains seven adsorbates, the model nitrogens bind directly on nickel atoms. Only in the case of three and four adsorbates is the nickel core structure that of structure 7.1 in bare  $\text{Ni}_7$ . The seventh adsorbate in structure (e) does not bind directly on a nickel atom, but rather straddles two of the adsorbed atoms. The energy difference between the structure with six and seven adsorbates is about 0.08 eV reflecting the weak binding between the seventh adsorbate and the remainder of the cluster [the cores of struc-

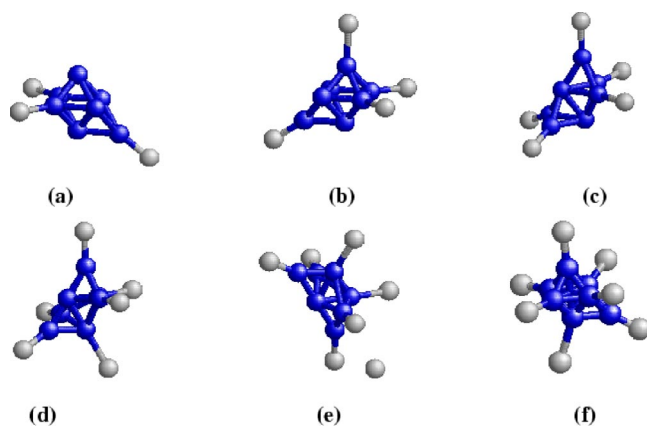


FIG. 8. The lowest energy structures of  $\text{Ni}_7$  with, respectively, 3–7 adsorbate atoms using model 2. The binding energies of each cluster relative to bare  $\text{Ni}_7$  and all adsorbates at infinity are (a) 1.3552 eV, (b) 1.7211 eV, (c) 1.9542 eV, (d) 2.0953 eV, (e) 2.1753 eV, and (f) 2.1329 eV. The core nickel structure with three and four adsorbates matches structure 7.1 of bare  $\text{Ni}_7$ , but with the adsorption of additional adsorbates, the core nickel structures differ from that observed in the bare nickel cluster. The seventh adsorbate [structure (e)] forms a weak bridge bond to two adjacent adsorbates rather than to nickel atoms. The 18th isomer of  $\text{Ni}_7$  with seven adsorbates is shown as structure (f), and is the only discovered structure having all seven adsorbates bound to all nickel atoms. Structure (f) has the same nickel core as structure 7.1 in bare  $\text{Ni}_7$ .

TABLE IV. The binding energies of some of the lowest energy isomers for the larger cluster sizes using model 2.

Cluster	Binding energy (eV)
10.1	1.3552
10.2	1.3537
10.3	1.3506
10.4	1.3466
11.1	1.7211
11.2	1.7090
11.3	1.6962
11.4	1.6871
12.1	1.9542
12.2	1.9440
12.3	1.9154
12.4	1.9151
13.1	2.0953
13.2	2.0896
13.3	2.0837
13.4	2.0821
14.1	2.1753
14.2	2.1723
14.3	2.1722
14.4	2.1664

tures (d) and (e) are similar]. With seven adsorbates, the only structure discovered with all seven model nitrogen molecules bound directly to the nickel atoms is shown as structure (f) which is the 18th isomer for the system. The nickel core in structure (f) has the capped octahedral structure characteristic of structure 7.1 in bare  $\text{Ni}_7$ .

In model 2, as with model 1, to save space we do not display the structures of all the discovered isomers for clusters having three or more adsorbates. We do list the binding energies of some of the lowest energy isomers in Table IV. To understand fully the structures of the potential energy surfaces in both models, we now examine the disconnectivity graphs<sup>13,14</sup> for  $\text{Ni}_7$  with and without a single adsorbate. Disconnectivity graphs have proved to be useful in understanding the potential surfaces for clusters and other systems having complex potential surfaces, and detailed discussions of their structure and interpretation can be found elsewhere.<sup>13</sup>

The disconnectivity graph for bare  $\text{Ni}_7$  is presented in Fig. 9. It is of interest to correlate the structures observed in Fig. 2 with the disconnectivity graph itself. As examples, isomers 7.1 and 7.6, which have similar structures, are directly connected with a small energy barrier. As another example, the structurally similar isomers 7.2 and 7.3 are directly connected with another small energy barrier. Structures 7.7 and 7.8 can be formed by small distortions of structures 7.2 and 7.3, and all four structures are found within the same portion of the disconnectivity graph. The energy differences and barriers between structures 7.1–7.18 are small, and these isomers appear connected in the same portion of Fig. 9 and are all associated with small energy barriers. We can describe such behavior as glassy. The glassy disconnectivity graph appearing in Fig. 9 is in contrast with what is observed in cluster systems with funnel energy landscapes<sup>18</sup> (e.g., the 13 and 38 particle Lennard-Jones clusters). Such funnel energy landscapes can exhibit solid to solid and solid to liquid like phase change phenomena and



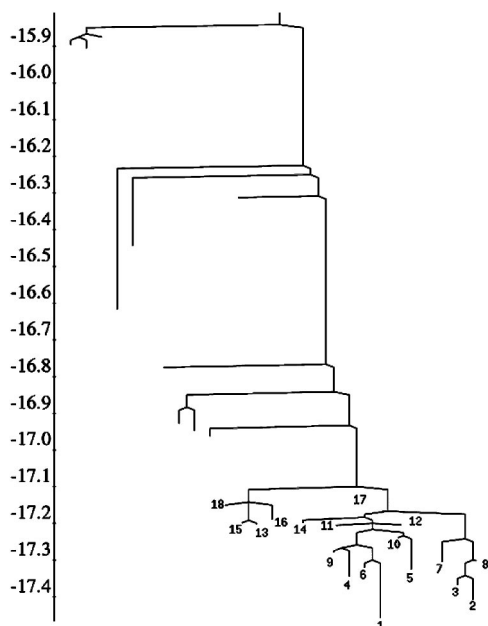


FIG. 9. The disconnectivity graph for bare  $\text{Ni}_7$  in the extended Hückel model. The ordinate axis displays the total energy of each cluster and the numbers label the lowest 18 minima.

can exhibit high temperature peaks in the heat capacity as a function of temperature.<sup>19</sup> In contrast glassy systems like  $\text{Ni}_7$  show rapid rises in the heat capacities at low temperatures.<sup>20</sup>

It is of interest to contrast the structure of the disconnectivity graph for  $\text{Ni}_7$  with graphs for the nickel cluster with adsorbates. We consider the changes for both models and a single adsorbate. Figure 10 is the disconnectivity graph for  $\text{Ni}_7$  with a single adsorbate using model 1 for the interaction potential between the nickel and the adsorbates. As with bare

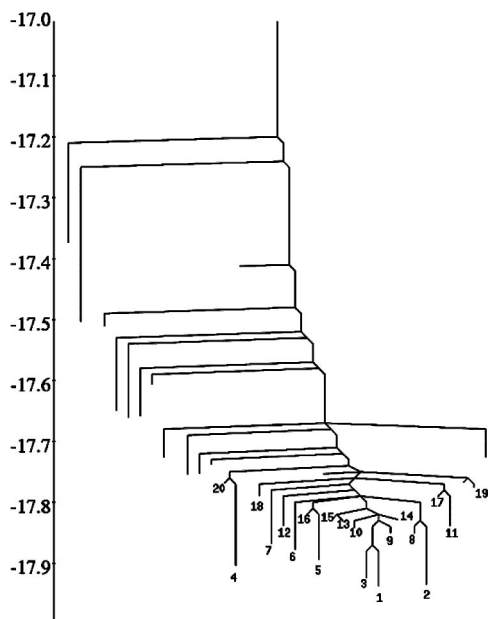


FIG. 10. The disconnectivity graph for  $\text{Ni}_7$  and a single molecular nitrogen adsorbate in model 1. The ordinate displays the total energy of each cluster. Only the 35 discovered structures that are lowest in energy are shown with the 20 lowest labeled in energy order.

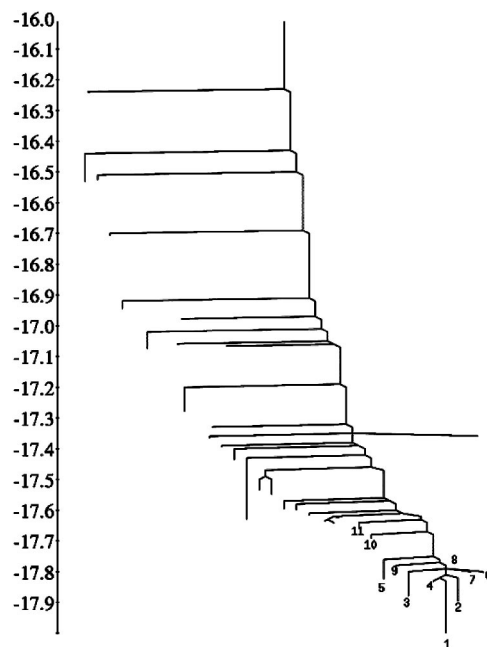


FIG. 11. The disconnectivity graph for  $\text{Ni}_7$  and a single molecular nitrogen adsorbate in model 2. The ordinate displays the total energy of each cluster. Only the 35 discovered structures that are lowest in energy are shown with the 11 lowest labeled in energy order.

$\text{Ni}_7$  it is useful to correlate the form of the disconnectivity graph with the structures displayed in Fig. 3. The closest connection between the global minimum shown as (a) in Fig. 3 is structure (c). The close connection between structures (a) and (c) at first is surprising considering the similarities between structures (a) and (f). However, on close examination of the structure of the transition state connecting (a) with (c), we find that the transition state structure is characterized by a modest modification of the core structure of (a). The adsorbate does not change its position significantly. In contrast, the transition state connecting structures (a) and (f) involves the motion of the adsorbate, and the energy of this transition state is higher than the transition state connecting structures (a) and (c). The disconnectivity graph shows many minima and transition states quite close in energy, and the system is clearly much glassier than observed in bare  $\text{Ni}_7$ . The glassy nature of this mixed system reflects similar observations in other mixed systems.<sup>21</sup>

In Fig. 11 we see the disconnectivity graph for  $\text{Ni}_7$  with a single adsorbate using model 2. As mentioned previously, the energy gap between the lowest energy isomer and the next adjacent isomer in energy is larger than the gap observed in model 1. These larger energy gaps are evident in Fig. 11 which is characteristic of a less glassy system. The closest link between the global minimum [structure (a) in Fig. 6] is the fourth isomer [structure (d) in Fig. 6]. All of the first nine isomers in model 2 are linked by low transition state barriers, and the disconnectivity graph has a funnel structure but with low energy barriers.

#### IV. DISCUSSION

It is evident that by using both potential models introduced in this work, the extended Hückel model for nickel

can change the isomer distribution from that found in the bare Ni<sub>7</sub> system by the adsorption of species having potential parameters qualitatively in agreement with those expected for molecular nitrogen adsorption. The lowest energy isomer for bare Ni<sub>7</sub> is a capped octahedron, and the capped octahedral core is found only with the addition of a single adsorbate in model 1 and with the addition of one, three, or four adsorbates in model 2. The reordering appears to be a consequence of the small energy differences between isomers for bare Ni<sub>7</sub> and the large size of the perturbation from the adsorbed molecules.

We have examined the disconnectivity graphs for bare Ni<sub>7</sub> as well as Ni<sub>7</sub> with a single adsorbate whose interaction with nickel is represented by both models 1 and 2. All three disconnectivity graphs have a glassy structure, with model 1 showing the lowest energy barriers between minima of the three cases studied. In studies of thermodynamic properties of such systems, low energy barriers produce a rapidly rising heat capacity at low temperatures. Such effects have been seen quantitatively in studies of the heat capacity of Ni<sub>7</sub><sup>20</sup> using the same potential model. The glassy structure of the potential energy surface results in significant structural modifications of the core nickel structures by adsorption.

In the experimental work of Parks *et al.*,<sup>3</sup> careful arguments are given to demonstrate that the inferred structures of bare nickel clusters are unchanged by the adsorption of nitrogen. The purpose of this work is not to refute those arguments. Our potential model is certainly not sufficiently accurate to claim that nitrogen induces significant isomer reordering in real nickel clusters. The imaginative nitrogen uptake technique is one of only a few experimental methods available to infer or determine the structures of small clusters. What we can claim is isomer reordering may prove to be important for systems with similar energetics, and a careful analysis is required in all such cases.

## ACKNOWLEDGMENTS

This work has been supported in part by National Science Foundation Grant Nos. CHE-0095053 and CHE-

0131114. We thank Professor Emanuele Curotto for providing us with the original extended Hückel code used to model the nickel–nickel interactions. We also thank Dr. M. Miller for helpful discussions and for his gracious assistance with respect to the preparation of the disconnectivity graphs in the current work.

- <sup>1</sup>D. Sabo, J. D. Doll, and D. L. Freeman, *J. Chem. Phys.* **118**, 7321 (2003).
- <sup>2</sup>D. Sabo, J. D. Doll, and D. L. Freeman, *J. Chem. Phys.* (to be published).
- <sup>3</sup>E. K. Parks, L. Zhu, J. Ho, and S. J. Riley, *J. Chem. Phys.* **100**, 7206 (1994).
- <sup>4</sup>E. K. Parks, G. C. Nieman, K. P. Kerns, and S. J. Riley, *J. Chem. Phys.* **108**, 3731 (1998).
- <sup>5</sup>J. Yoshinobu, R. Zenobi, J. Xu, Z. Xu, and J. T. Yates, Jr., *J. Chem. Phys.* **95**, 9393 (1991).
- <sup>6</sup>E. Curotto, A. Matro, D. L. Freeman, and J. D. Doll, *J. Chem. Phys.* **108**, 729 (1998).
- <sup>7</sup>M. E. Brubaker and M. Trenary, *J. Chem. Phys.* **85**, 6100 (1986).
- <sup>8</sup>D. J. Wales and J. P. K. Doye, *J. Phys. Chem. A* **101**, 5111 (1997).
- <sup>9</sup>W. H. Press, S. A. Teukolsky, W. T. Vetterling, and B. P. Flannery, *Numerical Recipes in Fortran 77: The Art of Scientific Computing*, 2nd ed. (Cambridge University Press, New York, 1992).
- <sup>10</sup>C. J. Tsai and K. D. Jordan, *J. Phys. Chem.* **97**, 11227 (1993).
- <sup>11</sup>E. B. Wilson, Jr., J. C. Decius, and P. C. Cross, *Molecular Vibrations* (Dover New York, 1980).
- <sup>12</sup>J. W. Ochterski, *Vibrational Analysis in Gaussian* (Gaussian, Inc., 1999), (<http://www.lct.jussieu.fr/manuals/Programmes/Gaussian98/vib.htm>)
- <sup>13</sup>O. M. Becker and M. Karplus, *J. Chem. Phys.* **106**, 1495 (1997).
- <sup>14</sup>J. P. K. Doye, M. A. Miller, and D. J. Wales, *J. Chem. Phys.* **111**, 8417 (1999).
- <sup>15</sup>D. M. Deaven and K. M. Ho, *Phys. Rev. Lett.* **75**, 288 (1995).
- <sup>16</sup>J. A. Niesse and H. R. Mayne, *J. Chem. Phys.* **105**, 4700 (1996).
- <sup>17</sup>D. L. Freeman and J. D. Doll, *Annu. Rev. Phys. Chem.* **47**, 43 (1996).
- <sup>18</sup>J. P. K. Doye, M. A. Miller, and D. J. Wales, *J. Chem. Phys.* **110**, 6896 (1999).
- <sup>19</sup>J. P. Neirotti, F. Calvo, D. L. Freeman, and J. D. Doll, *J. Chem. Phys.* **112**, 10340 (2000).
- <sup>20</sup>E. Curotto, D. L. Freeman, B. Chen, and J. D. Doll, *Chem. Phys. Lett.* **295**, 366 (1998).
- <sup>21</sup>L. J. Munro, A. Tharrington, and K. D. Jordan, *Comput. Phys. Commun.* **145**, 1 (2002).

The Journal of Chemical Physics is copyrighted by the American Institute of Physics (AIP). Redistribution of journal material is subject to the AIP online journal license and/or AIP copyright. For more information, see <http://ojps.aip.org/jcpo/jcpcr/jsp>  
Copyright of Journal of Chemical Physics is the property of American Institute of Physics and its content may not be copied or emailed to multiple sites or posted to a listserv without the copyright holder's express written permission. However, users may print, download, or email articles for individual use.

The Journal of Chemical Physics is copyrighted by the American Institute of Physics (AIP). Redistribution of journal material is subject to the AIP online journal license and/or AIP copyright. For more information, see <http://ojps.aip.org/jcpo/jcpcr/jsp>